Bull. Natl. Mus. Nat. Sci., Ser. C, 51, pp. 15–25, December 19, 2025

DOI: 10.50826/bnmnsgeopaleo.51.0_15

Confirming the Western Extension of the Hida Belt Beneath Mt. Daisen Volcano, SW Japan: Permian and Triassic Zircons of Gneiss and Granitoid Xenoliths Trapped in Quaternary Volcaniclastics in Inayoshi, Western Tottori

Yukiyasu Tsutsumi[1, 2*], Yukio Isozaki[3] and Keiji Kitani[4]

[1] Department of Science, National Museum of Nature and Science,
4–1–1 Amakubo, Tsukuba, Ibaraki 305–0005, Japan
[2] Graduate School of Life and Environment Sciences, University of Tsukuba,
1–1–1 Tennodai, Tsukuba, Ibaraki 305–8572, Japan
[3] Department of Eearth Science and Astronomy, University of Tokyo,
3–8–1 Komaba, Meguro-ku,Tokyo 153–8902, Japan
[4] Nishitani Engineering Consultant Co. Ltd.,
354–1 Yatsuya, Kurayoshi, Tottori 682–0025, Japan
*Author for correspondence: ytsutsu@kahaku.go.jp

Abstract The Hida belt in central Japan is a unique geotectonic unit characterized by granitoids of about 230-260 and 190 Ma, which are extremely rare elsewhere in Japan. The fragmentary occurrence of Jurassic Ebi granite in western Tottori prefecture, near Mt. Daisen and about 300 km to the west of the Hida belt, suggests a western extension of the Hida belt, but it is not yet confirmed. We collected three xenolith samples of granitoids and granitic gneiss within the Quaternary volcaniclastics in the Inayoshi area: two granodiorites (IY1 and IY4-1) and one gneiss (IY3-2). Newly obtained zircon U–Pb ages of about 230 Ma (Triassic) from samples IY1 and IY4-1 confirmed the first occurrence of pre-Jurassic granitoids, comparable with those from the Hida belt. The co-occurrence of Triassic and Jurassic granitoids positively suggests a western extension of the Hida belt in Inayoshi. As for IY3-2, the new U–Pb age of 245 Ma suggests a similarity to the coeval Hida gneiss associated with the Hida older granite. These age data and rock characteristics suggest that the Quaternary pyroclastics contain xenoliths of various rock types derived from the subsurface basement at different crustal levels, along which magma penetrated. The development of the western extension of the Hida belt is confirmed for the first time, about 300 km to the west, along the Japan Sea coast.
Key words: gneiss, granitoid, zircon, U–Pb age, Hida belt

Introduction

The Japanese Islands had evolved along an active continental margin, as recorded in the Paleozoic to Cenozoic accretionary complexes, their metamorphosed equivalents, and arc granitoids, until the separation from the Asian continent by the Miocene opening of the Japan Sea (a back-arc basin) (e.g., Isozaki *et al.*, 2010). The Hida belt in central Japan, composed of pre-Cretaceous granitoids and gneisses (e.g., Suwa, 1990), is quite distinct from all other geotectonic units in Japan. Its occurrence at the most continent-sided position in Japan (Fig. 1A) suggests an intimate connection to the pre-Japan Sea Asian margin. Recent zircon U-Pb dating confirmed that the Hida granitoids are two-fold in age: about 250–230 Ma for the older group and about 190 Ma for the younger (e.g., Kano, 1990; Kunugiza *et al.*, 2010; Takahashi *et al.*, 2018). The Hida gneiss, often associated with the older granitoids, was also analyzed; a paragneiss yielded U–Pb ages of detrital zircon ranging from 2000 to 250 Ma (Sano *et al.*, 2000) and those for metamorphic zircons of 247 Ma (Horie *et al.*, 2018). Thus, the gneiss was derived from the latest Permian to earliest Triassic sandstones, and was metamorphosed under high temperature conditions associated with coeval granitoid emplacement. On-land and marine geology around and within the Japan Sea suggests that the Hida belt forms a detached fragment of the Laoelin-Grodekov belt in the Russia, China, and North Korea border area, on the opposite side of the

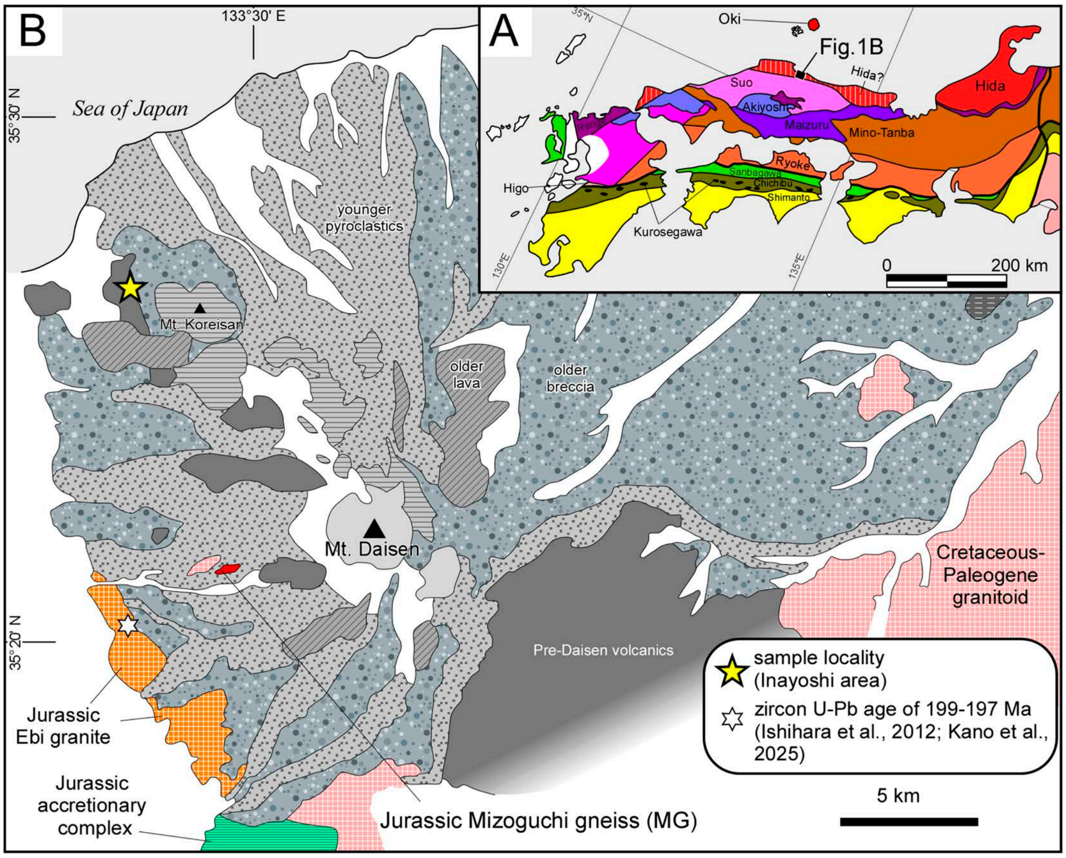

Fig. 1. Geological maps with sample locality. A: Geological unit map of western Japan. B: Geological map of western foothills of Mt. Daisen (modified, from Tsukui, 1984).

Japan Sea (Isozaki *et al.*, 2021, 2023, 2024). Nonetheless, the western extension of the Hida belt has not yet been clearly identified.

Extremely small-scale occurrences of pre-Cretaceous granitoids and gneissose rocks were reported in a narrow domain at Mizoguchi (Mizokuchi), near Mt. Daisen, a Miocene-Pleistocene volcano, dormant at present. The Rb–Sr whole rock-mineral isochron age (Jurassic) of the gneiss (Ishiga *et al.*, 1989), and zircon U–Pb age of 199–197 Ma of 'Ebi granite' from a neighboring area (Ishihara *et al.*, 2012; Kano *et al.*, 2025) suggest that the subsurface basement crust of Mt. Daisen may correspond to the younger Hida granitoid. However, the Jurassic gneisses from Mizoguchi (Mizoguchi gneiss: MG) clearly differ from the Triassic Hida gneiss in their trace element composition (Nozaka *et al.*, 2002) and detrital zircon age spectra (Tsutsumi *et al.*, 2017). Thus, correlation to the Hida belt remains unclear.

From Inayoshi town, about 10 km north of Mizoguchi (Fig. 1B), the occurrences of various xenoliths of undated granitoids and gneisses were reported from the Quaternary pyroclastics (Okada and Yamauchi, 2010). In order to check the claimed extension of the Hida belt in western Tottori prefecture, about 300 km to the west along the Japan Sea coast, we newly collected several samples of xenoliths (granitoids and gneisses) in Inayoshi for zircon U–Pb dating. This paper reports new ages of the Triassic granitoids for the first time from the area on the west of the Hida belt, and discusses the geotectonic implications in SW Japan.

Geological setting

Mizoguchi gneiss (MG) is composed of high-grade pelitic/psammitic, granitic and mafic gneisses, and a gneiss with a Jurassic Rb–Sr whole rock-mineral isochron age (Ishiga *et al.*, 1989, 1991). Ebi granite has zircon U–Pb ages of 198.6 ± 2.7 Ma and 197.4 ± 1.0 Ma (Ishihara *et al.*, 2012; Kano *et al.*, 2025), which are coeval to Hida granite (about 190 Ma and 230-260 Ma: e.g., Takahashi *et al.*, 2018). These Jurassic ages are used as a basis for correlating MG to the Hida belt. However, the interpretation of the geochemical data is that the MG was formed in the fore-arc region of an oceanic island arc, whereas the Hida gneiss was formed in a continental setting (Nozaka *et al.*, 2002). Moreover, zircon U–Pb dating revealed that the MG derived from Permo–Jurassic igneous-metamorphic rocks, with several Early Jurassic detrital zircon grains in a paragneiss sample (Tsutsumi *et al.*, 2017). These rocks were metamorphosed in the middle Jurassic; thus, younger than the Hida gneiss. Tsutsumi *et al.* (2017) concluded that the MG forms a northernmost part of the Phanerozoic subduction-accretion complex in Southwest Japan, clearly on the south of the non-accretionary Hida belt.

The Inayoshi area is over 10 km north of the locality of the MG (Fig. 1B). It is mostly covered with lavas from the Daisen volcano and volcaniclastics from the parasitic Koreisan lava dome. At the sampling locality in Inayoshi, many blocks of older-looking gneiss, amphibolite, and granitoid occur in a shallow gully (Okada and Yamauchi, 2010). Kano *et al.* (2025) identified these plutonic and metamorphic rocks as xenoliths incorporated within the Quaternary Koreisan pyroclastics.

Analytical methods

All sample preparations and analyses were conducted at National Museum of Nature and Science, Tsukuba, Japan. The rock samples were scrubbed and washed in an ultrasonic bath for ten minutes to avoid surface zircon contaminants as much as possible. Fragmentation of the rock samples was conducted by a high voltage pulse power selective fragmentation equipment, SELFRAG Lab (Selfrag AG). The zircon grains were handpicked from heavy fractions that were separated from heavy-liquid techniques. Zircon grains from the samples, the zircon standards FC1 (1099 Ma; Paces and Miller, 1993) and OD-3 (33 Ma; Iwano *et al.*, 2013), and the glass standard NIST SRM610 were mounted in an epoxy resin and polished till the surface was level with the center of the embedded grains. Before the mounting and polishing, secondary electron (SE) images of zircon grains are taken for morphological assessment. After mounting and polishing, backscattered electron and cathodoluminescence (CL) images of zircon grains were taken. A scanning electron microscope (SEM) -CL equipment, JSM-6610 (JEOL) and a CL detector (SANYU electron), was used for SE and CL images. The images were used to select suitable sites for analysis. U-Pb dating of these samples was carried out using a Laser Ablation Inductively Coupled Plasma Mass Spectrometer (LA-ICP-MS) that was composed of NWR213 (Elemental Scientific Lasers) and Agilent 7700x (Agilent Technologies). The experimental conditions and the analytical procedures for the measurements were after Tsutsumi *et al.* (2012), and additional devices of buffered type stabilizer (Tunheng and Hirata, 2004) and TwoVol2 sample cell were applied. The spot size of the laser was 25 µm. A correction for common Pb was made on the basis of the measured $^{207}Pb/^{206}Pb$ ratio (^{207}Pb correction), and $^{208}Pb/^{206}Pb$ and Th/U ratios (^{208}Pb correction) (e.g., Williams, 1998) and the model for common Pb compositions proposed by Stacey and Kramers (1975). In this paper, we adopt ^{207}Pb correction for age discussion because it is effective in calculating Phanerozoic ^{238}U-$^{206}Pb^{*}$ age compared with ^{208}Pb correction (e.g., Williams, 1998). $^{238}U/^{206}Pb^{*}$ and $^{207}Pb^{*}/^{206}Pb^{*}$ ratios which corrected by ^{208}Pb correction are used for the concordia plot. Pb^{*} indicates radiometric Pb. The pooled ages presented in this study were calculated using Isoplot/Ex software which statistically rejection functionality was enabled (Ludwig, 2012). The data of secondary standard OD-3 zircon obtained during analysis yielded weighted mean ages of 31.0 ± 0.4 Ma (n = 9; MSWD = 0.37; when IY1 and IY4-1 were analyzed), and 31.2 ± 0.7 Ma (n = 6; MSWD = 0.46; when IY3-2 was analyzed). MSWD is acronym of mean square weighted deviation, which is calculated from square root of χ^2 value.

Sample descriptions and results of zircon age analysis

For zircon U–Pb geochronology, we collected three rock samples (IY1, IY3-2, and IY4-1). All three yielded datable zircon grains. Brief descriptions of these rocks are given below. These samples were collected from different localities, but the localities are within the precision range of a handheld GPS device around the point (lat: N 35°26′47.7″, long: E 133°27′26.5″). All rock samples are stored at the National Museum of Nature

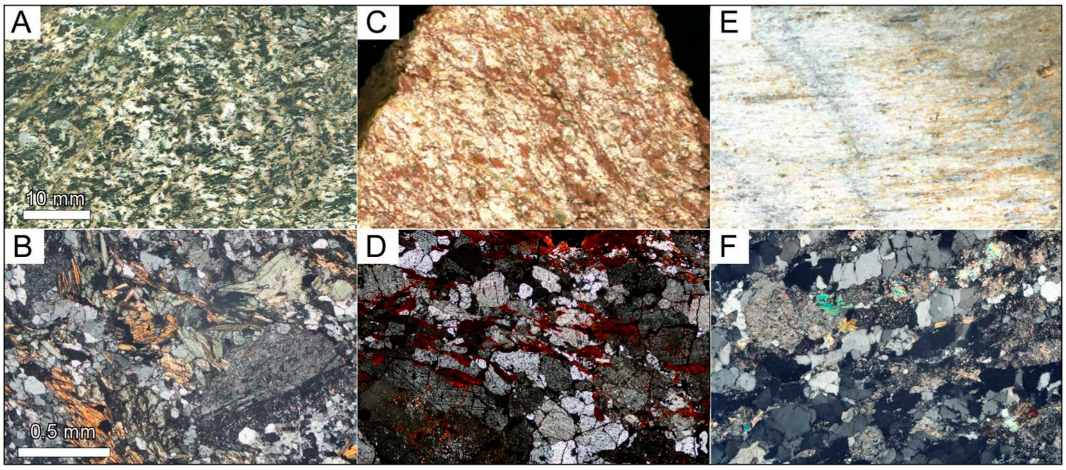

Fig. 2. Photograph of the samples and photomicrograph of the samples in thin sections. A and B: IY1 (altered granodiorite), C and D: IY4-1 (altered granodiorite), E and F: IY3-2 (leucocratic granitic gneiss).

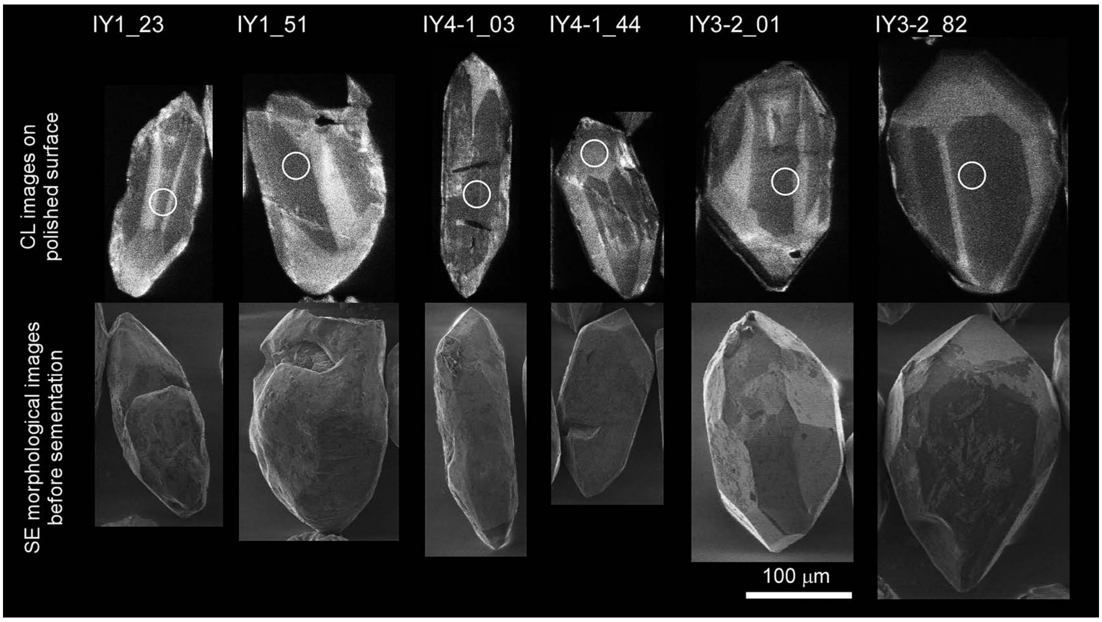

Fig. 3. Morphological secondary electron (SE) images before cement in resin and cathodoluminescence (CL) images of analyzing section of typical zircon grains from the samples. Circles on the images indicate spots analyzed by LA-ICP-MS. Spot diameter is 25 μm approx.

and Science. The registration number of each sample is the catalogue number of the rock specimen in the collection database of the National Museum of Nature and Science (http://db.kahaku.go.jp/webmuseum_en/).

Table A1 lists zircon data in terms of the fraction of common ^{206}Pb, U, and Th concentrations, Th/U, ^{238}U/^{206}Pb* and ^{207}Pb*/^{206}Pb* ratios, and radiometric ^{238}U–^{206}Pb* ages of the samples. All errors are of 1 sigma level. Errors of weighted mean zircon U–Pb ages are at a 95% confidence interval (95% conf.). Concordia diagrams for each sample are shown in Fig. 4.

IY1: altered granodiorite

A medium-grained, dark-colored granodiorite with indistinct foliation (Fig. 2A). It consists of quartz, plagioclase, K-feldspar and biotite. K-feldspar are replaced by fine-grained plagioclase, muscovite and biotite. Original biotite in the granodiorite is completely replaced by secondary minerals (Fig. 2B). The registration number is 137271.

Most zircon grains are partly rounded and are 80 to 230 μm in length, with elongation ratios of 1.2 to 4.3. CL images of the grains show indistinct oscillatory zoning and distinct sector zoning, but no metamorphic rim is observed (Fig. 3A, B). A total of 74

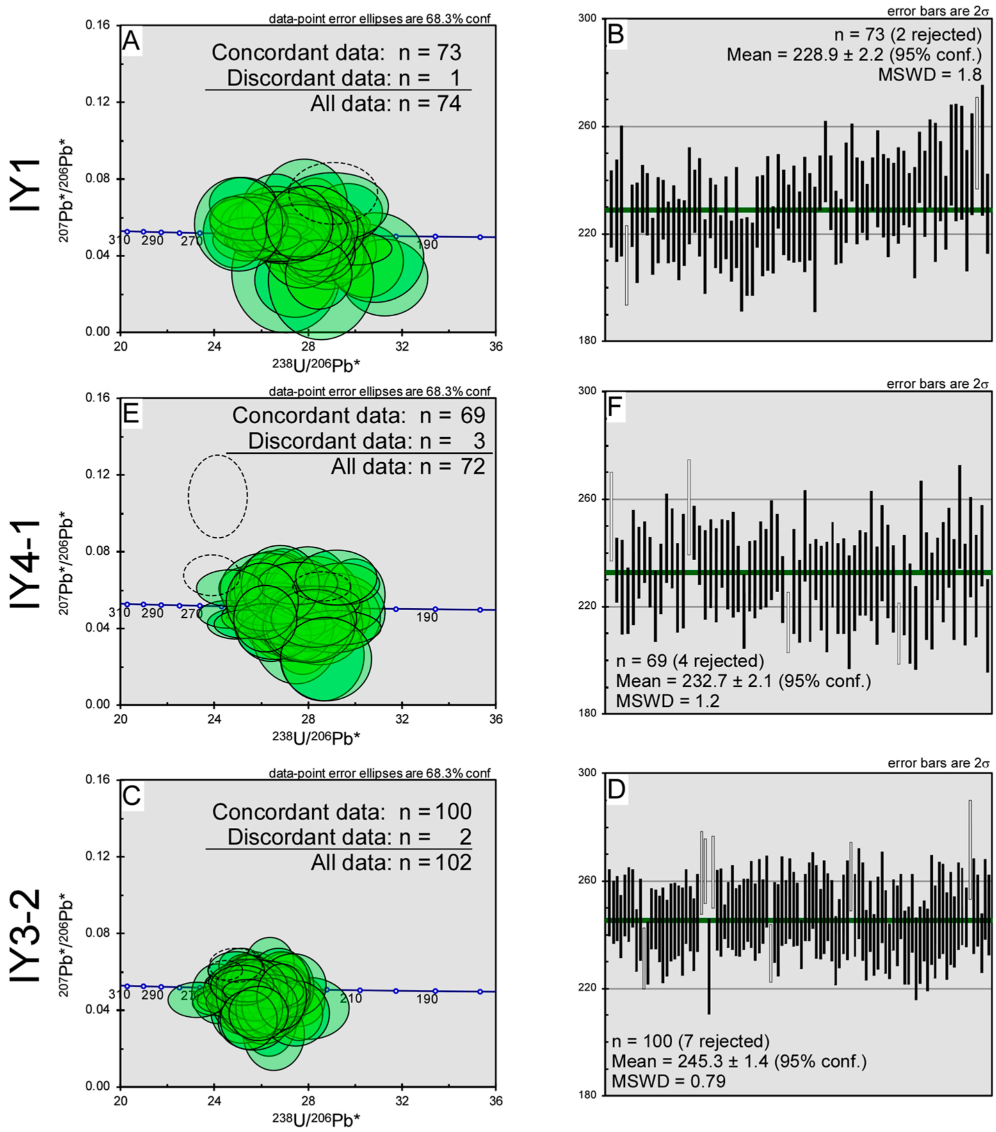

Fig. 4. Tera–Wasserberg U–Pb concordia diagrams and age distribution plot of the samples. A and B: IY1 (altered granodiorite), C and D: IY4-1 (altered granodiorite), E and F: IY3-2 (leucocratic granitic gneiss). ^{207}Pb* and ^{206}Pb* indicate radiometric ^{207}Pb and ^{206}Pb, respectively.

spots from 74 grains were analyzed, and 73 were concordant. Concordant data indicate 208–254 Ma. After two data items were excluded, the weighted mean age of 71 data items was 228.9 ± 2.2 Ma (MSWD = 1.8; Fig. 4A, B).

IY4-1: altered granodiorite

A medium-grained, reddish-colored granodiorite with indistinct foliation (Fig. 2C). It is of the same constitution as IY1, but with a complete replacement of the original biotite and/or secondary minerals by fine-grained reddish opaque minerals (Fig. 2D). The registration number is 137276.

Most zircon grains are partly rounded and are 90 to 210 μm in length, with elongation ratios of 1.4 to 3.4. CL images of the grains show indistinct oscillatory zoning and distinct sector zoning, but no metamorphic rim is observed (Fig. 3C, D). A total of 72 spots from 72 grains were analyzed, and 69 were concordant. Concordant data indicate 217–257 Ma. After four data items were excluded, the weighted mean age of 65 data items was 232.7 ± 2.1 Ma (MSWD = 1.2; Fig. 4C, D).

IY3-2: leucocratic granitic gneiss

A well-foliated leucocratic granitic gneiss (Fig. 2E), with an elongation of quartz and an alignment of biotite flakes. Biotite, plagioclase, K-feldspar and quartz occur as major phases. The original biotite of the gneiss is mostly replaced by secondary minerals (Fig. 2F). The registration number is 137274.

Most zircon grains are partly rounded and are 110 to 340 μm in length, with elongation ratios of 1.2 to 4.1. CL images of the grains show indistinct oscillatory zoning and distinct sector zoning, but no metamorphic rim is observed (Fig. 3E, F). A total of 102 spots from 102 grains were analyzed, and 100 were concordant. Concordant data indicate 228–272 Ma. After seven data items were excluded, the weighted mean age of 93 data items was 245.3 ± 1.4 Ma (MSWD = 0.79; Fig. 4E, F).

Discussion

New zircon U-Pb ages of the two granodiorite samples IY1 and IY4-1, of about 230 Ma, correspond to those of the Hida older granite (about 250–230 Ma, Permo–Triassic: Takahashi *et al.*, 2018). This is the first finding of Triassic granite in western Tottori, about 300 km west of the Hida belt. The protolith of granitic gneiss sample IY3-2 with 245 Ma zircon may correspond to the Hida older granite, as well as the previously reported orthogneiss of the MG (258 Ma: Tsutsumi *et al.*, 2017). The age of the high-grade metamorphism is not well constrained, but the gneissose rocks in the Inayoshi-Mizoguchi area may derive from the Jurassic high-*T* type metamorphic complex of the Hida belt.

In addition to the previously reported Jurassic Ebi granite (197–199 Ma: Ishihara *et al.*, 2012; Kano *et al.*, 2025) corresponding to the Hida younger granite (about 190 Ma: Takahashi *et al.*, 2018), this study newly confirms the occurrence of Triassic granitoids from the neighboring area in western Tottori. The co-occurrence of the Triassic and Jurassic granitoids have not been known elsewhere in Japan but only in the Hida belt, positively suggesting that the western extension of the Hida belt occurs beneath Mt. Daisen.

Acknowledgments

The authors thank Mrs. Y. Kusaba of the National Museum of Nature and Science for her help in SEM analysis. A part of this work was supported by JSPS KAKENHI Grant Number 24K07169 and by a program of the National Museum of Nature and Science: “Collection building of granitoids in Southwest Japan and elucidation the peculiarities of their age distribution”.

References

Hattori, H. and Katada, M. (1961) *Geology of the Neu District*. Quadrangle Series, 1 : 50,000, Geological Survey of Japan. 63 p. (in Japanese with English abstract).

Horie, K., Tsutsumi, Y., Takehara, M. and Hidaka, H. (2018) Timing and duration of regional metamorphism in the Kagasawa and Unazuki areas, Hida metamorphic complex, southwest Japan. *Chemical Geology*, **484**: 148–167.

Ishiga, H., Sugawara, M. and Iizumi, S. (1991) The Ebi Tectonic Zone, Late Paleozoic suture of the southern margin of the Hida Belt in Kofu-cho, southwest of Mt. Daisen, southwest Japan. *Geological reports of Shimane University,* **10**: 53–56 (in Japanese with English abstract).

Ishiga, H., Suzuki, M., Iizumi, S., Nishimura, K., Kagami, H. and Tanaka, S. (1989) Western extension of Hida terrane: with special reference to gneisses and mylonites discovered in Mizoguchi-cho, western part of Daisen, Tottori Prefecture, southwest Japan. *Journal of the Geological Society of Japan* **95**: 129–132 (in Japanese).

Ishihara, S., Hirano, H. and Tani, K. (2012) Jurassic granitoids intruding into the Hida and Sangun metamorphic rocks in the central Sanin District, Japan. *Bulletin of the Geological Survey of Japan* **63**: 227–231 (in Japanese with English abstract).

Isozaki, Y., Aoki, K., Nakama, T. and Yanai, S. (2010) New insight into a subduction-related orogen: A reappraisal of the geotectonic framework and evolution of the Japanese Islands. *Gondwana Research,* **18**: 82–105.

Isozaki, Y., Hasegawa, R., Nakano, T., Tsutsumi, Y., Nechaev, V., Zakharov, Y. and Popov, A. (2021). Zircon U–Pb ages of Permian–Triassic granitoids in the southeastern Laoelin-Grodekov belt, Primorye, Far East Russia: Possible correlation with the Hida belt in Central Japan. *Bulletin of National Museum of Nature and Science Series C*, **47**: 25–39.

Isozaki, Y., Iwano, H., Sawaki, Y., Kunugiza, K. and Hirata, T. (2024) Origin of the Hida belt, central Japan, with respect to the Late Triassic granitoids-bearing Cretaceous provenance: U–Pb Dating and trace element geochemistry of detrital zircons in Tetori sandstones. *Journal of Geography (Chigaku Zasshi)*, **133**, 195–218 (in Japanese with English abstract).

Isozaki, Y., Sawaki, Y., Iwano, H., Hirata, T. and Kunugiza, K. (2023) Late Triassic A-type granite boulders in Lower Cretaceous conglomerate of the Hida belt, Japan: origin and bearing on the Yamato Tectonic Line in Far East Asia. *Island Arc*, **32**: e12475.

Iwano, H., Orihashi, Y., Hirata, T., Ogasawara, M., Danhara, T., Horie, K., Hasebe, N., Sueoka, S., Tamura, A., Hayasaka, Y., Katsube, A., Ito, H., Tani, K., Kimura, J., Chang, Q., Kouchi, Y., Haruta, Y. and Yamamoto, K. (2013) An inter-laboratory evaluation of OD-3 zircon for use as a secondary U–Pb dating standard. *Island Arc* **22**: 382–394.

Kano, K., Matsuura, H., Nakano, S. and Yamauchi, S (2025) *Geology of the Yonago District, 2nd Ed*. Quadrangle Series, 1 : 50,000, Geological Survey of Japan, AIST, 84 p. (in Japanese with English abstract).

Kano, T. (1990) Granitic rocks in the Hida complex. *Mining Geology*, **40**: 397–413 (in Japanese with English abstract).

Kunugiza, K., Shimizu, M. and Otoh, S. (2010) U–Th–Pb chronological constraints on the geotectonic history of Central Japan from the Hida metamorphism through the opening of Japan Sea to the present. *Journal of the Geological Society of Japan*, **116 (supplement)**: 83–101 (in Japanese with English abstract).

Ludwig, K. R. (2012) Isoplot 3.75-4.15: a geochronological toolkit for Microsoft Excel. In: *Berkeley Geochronology Center Special Publication*, Berkeley, California.

Nozaka, T., Masunari, H. and Tamiya, S. (2002) Geochemistry of metamorphic rocks from Mizoguchi, western Tottori Prefecture, Japan and its geological significance. *Journal of Mineralogical and Petrological Sciences*, **97**: 227–237.

Okada, R. and Yamauchi, S. (2010) Geology of the Yodoe area, northwestern foothill of Mt. Daisen. *News Letter of Shimane Earth Science Association*, **25**: 11–15 (in Japanese)*.

Paces, J. B. and Miller, J. D. (1993) Precise U–Pb age of Duluth Complex and related mafic intrusions, northern Minnesota: geochronological insights to physical, petrogenetic, paleomagnetic, and tectonomagmatic processes associated with the 1.1 Ga midcontinent rift system. *Journal of Geophysical Research,* **98**: 13997–14013.

Sano, Y., Hidaka, H., Terada, K., Shimizu, H. and Suzuki, M. (2000) Ion microprobe U-Pb zircon geochronology of the Hida gneiss: Finding of the oldest minerals in Japan. *Geochemical Journal,* **34**: 135–153.

Stacey, J. S. and Kramers, J. D. (1975) Approximation of terrestrial lead isotope evolution by a two–stage model. *Earth and Planetary Science Letters*, **26**: 207–221.

Suwa, K. (1990) Hida-Oki Terrane. In: Ichikawa, K., Mizutani, S., Hara, I., Hada, S. and Yao, A. (Ed.), Pre-Cretaceous terranes of Japan. Publication of IGCP Project No. 224: Pre-Jurassic evolution of eastern Asia. Nippon Insatsu Shuppan, Osaka, pp. 13–24.

Takahashi, Y., Cho, D.-L., Mao, J., Zhao, X. and Yi, K. (2018) SHRIMP U–Pb zircon ages of the Hida metamorphic and plutonic rocks, Japan: Implications for late Paleozoic to Mesozoic tectonics around the Korean Peninsula. *Island Arc*, **27**: e12220.

Tsukui, M. 1984. Geology of Daisen Volcano. *Journal of the Geological Society of Japan*, **90**, 643–658 (in Japanese with English abstract).

Tsutsumi, Y., Horie, K., Sano, T., Miyawaki, R., Momma, K., Matsubara, S., Shigeoka, M. and Yokoyama, K. (2012) LA–ICP–MS and SHRIMP ages of zircons in chevkinite and monazite tuffs from the Boso Peninsula, Central Japan. *Bulletin of the National Museum of Nature and Science, Series C*, **38**: 15–32.

Tsutsumi, Y., Isozaki, Y. and Terabayashi, M. (2017) The most continent-sided occurrence of the Phanerozoic subduction-related orogens in SW Japan: zircon U–Pb dating of the Mizoguchi gneiss on the western foothill of Mt. Daisen volcano in Tottori. *Journal of Asian Earth Sciences*, **145**: 530–541.

Tunheng, A and Hirata, T. (2004) Development of signal smoothing device for precise elemental analysis using laser ablation-ICP-mass spectrometry. *Journal of Analytical Atomic Spectrometry*, **7**: 932–934.

Williams, I. S. (1998) U–Th–Pb geochronology by ion microprobe. In McKibben, M. A., Shanks, W. C. P. and Ridley, W. I. (Eds.), *Applications of Microanalytical Techniques to Understanding Mineralizing Processes*. Reviews in Economic Geology 7, Society of Economic Geologists, Littleton, CO. USA, pp. 1–35.

* English translation from the original written in Japanese.

Table A1. LA-ICP-MS U-Pb data and calculated ages of zircons in the samples.

Labels	$^{206}Pb_c$ (1) (%)	U (ppm)	Th (ppm)	Th/U	$^{238}U/^{206}Pb^*$ (1)	$^{207}Pb^*/^{206}Pb^*$ (1)	$^{238}U/^{206}Pb^*$ age (1) (Ma)	$^{238}U/^{206}Pb^*$ age (2) (Ma)	Remarks
IY1_001	0.01	59	47	0.82	27.48 ± 0.90	0.0541 ± 0.0113	230.5 ± 7.4	229.5 ± 7.2	
IY1_002	0.00	34	18	0.54	27.67 ± 1.17	0.0415 ± 0.0075	228.9 ± 9.5	228.9 ± 9.5	
IY1_003	0.77	22	12	0.54	27.01 ± 1.53	0.0313 ± 0.0208	234.4 ± 13.0	236.2 ± 12.2	
IY1_004	2.56	60	47	0.80	31.23 ± 1.21	0.0286 ± 0.0133	203.2 ± 7.7	208.4 ± 7.4	
IY1_005	0.00	106	57	0.55	27.91 ± 0.72	0.0454 ± 0.0034	227.0 ± 5.7	227.0 ± 5.7	
IY1_006	0.15	31	15	0.49	28.66 ± 1.24	0.0520 ± 0.0124	221.1 ± 9.4	220.7 ± 9.3	
IY1_007	0.00	64	53	0.86	27.15 ± 0.74	0.0472 ± 0.0050	233.2 ± 6.3	233.2 ± 6.3	
IY1_008	0.01	157	158	1.03	27.19 ± 0.71	0.0564 ± 0.0078	232.8 ± 5.9	231.2 ± 5.7	
IY1_009	1.82	117	119	1.04	29.67 ± 0.78	0.0433 ± 0.0102	213.7 ± 5.5	215.6 ± 5.2	
IY1_010	0.02	51	44	0.88	28.09 ± 1.07	0.0515 ± 0.0136	225.5 ± 8.4	225.3 ± 8.0	
IY1_011	0.27	136	134	1.01	27.68 ± 0.71	0.0491 ± 0.0080	228.8 ± 5.7	229.2 ± 5.5	
IY1_012	2.68	83	76	0.93	28.26 ± 0.76	0.0632 ± 0.0115	224.2 ± 6.0	220.8 ± 5.7	
IY1_013	0.26	76	38	0.52	28.14 ± 0.90	0.0545 ± 0.0085	225.1 ± 7.1	224.1 ± 7.0	
IY1_014	0.00	60	49	0.84	29.00 ± 1.00	0.0522 ± 0.0063	218.5 ± 7.4	218.1 ± 7.6	
IY1_015	1.68	102	80	0.81	29.13 ± 0.85	0.0397 ± 0.0094	217.6 ± 6.3	220.5 ± 6.1	
IY1_016	1.39	40	31	0.80	27.40 ± 1.13	0.0275 ± 0.0129	231.1 ± 9.4	234.3 ± 9.0	
IY1_017	0.24	115	118	1.05	27.24 ± 0.72	0.0508 ± 0.0084	232.4 ± 6.0	232.4 ± 5.8	
IY1_018	0.59	53	27	0.51	27.38 ± 1.11	0.0549 ± 0.0101	231.2 ± 9.2	230.1 ± 9.1	
IY1_019	2.33	79	65	0.83	30.43 ± 1.04	0.0372 ± 0.0127	208.4 ± 7.0	211.8 ± 6.9	
IY1_020	1.52	125	118	0.97	27.91 ± 0.72	0.0405 ± 0.0092	227.0 ± 5.8	229.8 ± 5.5	
IY1_021	2.22	57	44	0.79	28.77 ± 1.03	0.0405 ± 0.0118	220.3 ± 7.7	223.1 ± 7.7	
IY1_022	0.00	105	93	0.90	29.30 ± 0.72	0.0505 ± 0.0041	216.3 ± 5.2	216.3 ± 5.4	
IY1_023	0.00	58	46	0.80	27.90 ± 0.93	0.0533 ± 0.0059	227.0 ± 7.5	226.3 ± 7.6	
IY1_024	0.00	124	112	0.92	29.45 ± 0.77	0.0563 ± 0.0050	215.3 ± 5.5	213.7 ± 5.6	
IY1_025	0.00	31	21	0.68	28.00 ± 1.18	0.0458 ± 0.0072	226.2 ± 9.4	226.2 ± 9.4	
IY1_026	1.33	49	35	0.73	30.81 ± 1.35	0.0391 ± 0.0154	205.9 ± 8.9	208.6 ± 8.5	
IY1_027	0.00	68	54	0.81	29.95 ± 1.04	0.0438 ± 0.0057	211.8 ± 7.2	211.8 ± 7.2	
IY1_028	0.37	71	51	0.74	29.64 ± 0.97	0.0628 ± 0.0101	213.9 ± 6.9	210.7 ± 6.7	
IY1_029	0.93	91	78	0.87	27.99 ± 0.86	0.0395 ± 0.0094	226.3 ± 6.8	228.4 ± 6.6	
IY1_030	0.57	54	39	0.75	27.78 ± 1.21	0.0677 ± 0.0150	228.0 ± 9.8	223.2 ± 9.3	
IY1_031	2.47	29	18	0.65	28.51 ± 1.48	0.0270 ± 0.0204	222.2 ± 11.3	227.8 ± 10.6	
IY1_032	0.29	127	107	0.86	29.01 ± 0.86	0.0522 ± 0.0089	218.4 ± 6.4	218.0 ± 6.2	
IY1_033	1.54	113	103	0.93	26.65 ± 0.84	0.0555 ± 0.0119	237.5 ± 7.4	236.2 ± 6.9	
IY1_034	0.00	66	57	0.89	27.58 ± 0.95	0.0551 ± 0.0057	229.6 ± 7.8	228.3 ± 7.9	
IY1_035	1.78	93	83	0.92	28.53 ± 0.94	0.0419 ± 0.0101	222.1 ± 7.2	224.5 ± 7.0	
IY1_036	0.00	47	36	0.78	27.53 ± 1.08	0.0594 ± 0.0073	230.0 ± 8.9	227.6 ± 9.0	
IY1_037	0.92	104	99	0.98	28.56 ± 0.90	0.0466 ± 0.0115	221.8 ± 6.9	222.9 ± 6.6	
IY1_038	0.00	53	39	0.75	27.70 ± 1.30	0.0551 ± 0.0077	228.6 ± 10.5	227.4 ± 10.7	
IY1_039	0.00	58	41	0.72	27.69 ± 0.97	0.0582 ± 0.0074	228.7 ± 7.9	226.6 ± 8.1	
IY1_040	0.00	21	11	0.52	29.02 ± 1.55	0.0657 ± 0.0117	218.4 ± 11.4	214.3 ± 11.7	
IY1_041	0.00	150	160	1.09	26.44 ± 0.57	0.0502 ± 0.0033	239.3 ± 5.0	239.3 ± 5.0	
IY1_042	0.00	96	60	0.64	25.59 ± 0.79	0.0482 ± 0.0038	247.1 ± 7.5	247.1 ± 7.5	
IY1_043	0.00	74	68	0.95	26.88 ± 0.81	0.0479 ± 0.0052	235.5 ± 6.9	235.5 ± 6.9	
IY1_044	0.00	37	27	0.74	29.02 ± 1.25	0.0726 ± 0.0106	218.4 ± 9.2	212.4 ± 9.4	discordant
IY1_045	0.00	106	96	0.94	28.12 ± 0.86	0.0603 ± 0.0058	225.3 ± 6.7	222.6 ± 6.9	
IY1_046	0.70	120	119	1.02	28.59 ± 0.82	0.0518 ± 0.0096	221.7 ± 6.3	221.3 ± 6.0	
IY1_047	0.83	55	22	0.42	26.55 ± 1.07	0.0606 ± 0.0104	238.3 ± 9.4	235.5 ± 9.3	
IY1_048	0.00	58	47	0.83	25.63 ± 0.76	0.0476 ± 0.0042	246.7 ± 7.2	246.7 ± 7.2	
IY1_049	0.00	50	37	0.76	27.23 ± 0.96	0.0496 ± 0.0068	232.5 ± 8.0	232.5 ± 8.0	
IY1_050	0.00	82	63	0.79	27.04 ± 0.78	0.0443 ± 0.0046	234.1 ± 6.6	234.1 ± 6.6	
IY1_051	0.66	70	60	0.88	27.92 ± 0.70	0.0438 ± 0.0100	226.9 ± 5.6	228.4 ± 5.2	
IY1_052	0.36	161	189	1.20	26.60 ± 0.60	0.0483 ± 0.0078	237.9 ± 5.3	238.7 ± 5.0	
IY1_053	0.00	44	34	0.78	26.06 ± 0.96	0.0575 ± 0.0074	242.7 ± 8.8	240.8 ± 9.0	
IY1_054	0.00	48	41	0.88	26.57 ± 0.94	0.0638 ± 0.0126	238.1 ± 8.3	234.4 ± 7.8	
IY1_055	1.43	37	20	0.54	27.69 ± 1.13	0.0458 ± 0.0149	228.7 ± 9.1	230.1 ± 9.2	
IY1_056	0.00	78	60	0.78	27.01 ± 0.78	0.0554 ± 0.0044	234.3 ± 6.6	233.1 ± 6.7	
IY1_057	0.00	39	19	0.50	27.00 ± 1.04	0.0471 ± 0.0065	234.4 ± 8.9	234.4 ± 8.9	
IY1_058	0.00	98	53	0.55	26.67 ± 0.79	0.0448 ± 0.0042	237.3 ± 6.9	237.3 ± 6.9	
IY1_059	0.00	143	162	1.16	27.06 ± 0.57	0.0552 ± 0.0034	234.0 ± 4.9	232.7 ± 4.9	
IY1_060	0.66	34	18	0.55	28.11 ± 1.30	0.0543 ± 0.0147	225.4 ± 10.3	224.4 ± 10.2	
IY1_061	0.00	88	68	0.79	25.81 ± 0.70	0.0453 ± 0.0043	245.0 ± 6.6	245.0 ± 6.6	
IY1_062	0.00	63	51	0.82	26.91 ± 0.92	0.0431 ± 0.0048	235.2 ± 7.9	235.2 ± 7.9	
IY1_063	0.00	54	44	0.83	25.48 ± 0.83	0.0570 ± 0.0077	248.2 ± 7.9	246.4 ± 8.2	

Table A1. Continued.

Labels	$^{206}Pb_c$ (1) (%)	U (ppm)	Th (ppm)	Th/U	$^{238}U/^{206}Pb^*$ (1)	$^{207}Pb^*/^{206}Pb^*$ (1)	$^{238}U/^{206}Pb^*$ age (1) (Ma)	$^{238}U/^{206}Pb^*$ age (2) (Ma)	Remarks
IY1_064	0.00	21	10	0.50	26.72 ± 1.43	0.0551 ± 0.0121	236.8 ± 12.4	235.6 ± 12.9	
IY1_065	0.00	85	73	0.88	26.38 ± 0.83	0.0494 ± 0.0047	239.9 ± 7.4	239.9 ± 7.4	
IY1_066	2.21	76	67	0.90	28.39 ± 0.94	0.0301 ± 0.0120	223.1 ± 7.3	228.1 ± 6.9	
IY1_067	0.00	44	35	0.81	25.34 ± 0.97	0.0488 ± 0.0075	249.5 ± 9.3	249.5 ± 9.3	
IY1_068	0.00	38	29	0.79	25.43 ± 1.09	0.0574 ± 0.0099	248.6 ± 10.5	246.7 ± 10.8	
IY1_069	0.00	52	43	0.86	25.38 ± 1.08	0.0593 ± 0.0076	249.2 ± 10.4	246.7 ± 10.6	
IY1_070	0.00	37	26	0.72	27.59 ± 1.34	0.0531 ± 0.0089	229.5 ± 11.0	228.8 ± 11.2	
IY1_071	0.00	41	27	0.69	25.16 ± 0.94	0.0675 ± 0.0089	251.2 ± 9.2	246.2 ± 9.5	
IY1_072	1.48	89	80	0.92	24.84 ± 0.88	0.0524 ± 0.0123	254.4 ± 8.9	254.1 ± 8.5	
IY1_073	0.21	30	17	0.57	24.99 ± 1.24	0.0564 ± 0.0161	252.9 ± 12.3	251.3 ± 12.1	
IY1_074	0.39	65	58	0.92	27.60 ± 0.94	0.0569 ± 0.0127	229.5 ± 7.6	227.7 ± 7.4	
IY3-2_001	0.08	42	33	0.81	25.08 ± 0.67	0.0441 ± 0.0087	252.0 ± 6.6	252.2 ± 6.2	
IY3-2_002	0.67	48	35	0.75	25.55 ± 0.62	0.0476 ± 0.0078	247.5 ± 5.9	248.6 ± 5.8	
IY3-2_003	0.19	42	35	0.84	25.34 ± 0.67	0.0470 ± 0.0090	249.5 ± 6.4	250.0 ± 6.0	
IY3-2_004	0.00	41	21	0.53	25.73 ± 0.61	0.0594 ± 0.0046	245.8 ± 5.7	243.3 ± 5.8	
IY3-2_005	0.00	63	30	0.48	25.17 ± 0.59	0.0484 ± 0.0031	251.1 ± 5.7	251.1 ± 5.7	
IY3-2_006	0.00	37	27	0.76	25.08 ± 0.68	0.0528 ± 0.0047	252.0 ± 6.7	251.5 ± 6.9	
IY3-2_007	0.00	54	34	0.64	24.91 ± 0.55	0.0498 ± 0.0045	253.8 ± 5.5	253.8 ± 5.5	
IY3-2_008	0.00	86	29	0.34	24.43 ± 0.50	0.0609 ± 0.0035	258.7 ± 5.2	255.6 ± 5.2	discordant
IY3-2_009	0.00	44	30	0.69	26.43 ± 0.62	0.0554 ± 0.0050	239.4 ± 5.5	238.1 ± 5.7	
IY3-2_010	0.00	30	19	0.65	25.74 ± 0.81	0.0502 ± 0.0069	245.7 ± 7.6	245.7 ± 7.6	
IY3-2_011	1.69	56	39	0.72	27.56 ± 0.71	0.0448 ± 0.0087	229.7 ± 5.8	231.4 ± 5.7	
IY3-2_012	0.00	45	35	0.80	27.13 ± 0.68	0.0506 ± 0.0044	233.3 ± 5.8	233.3 ± 5.8	
IY3-2_013	0.95	45	34	0.78	25.90 ± 0.63	0.0443 ± 0.0090	244.2 ± 5.9	246.3 ± 5.7	
IY3-2_014	0.00	54	41	0.77	25.71 ± 0.59	0.0502 ± 0.0039	246.0 ± 5.5	246.0 ± 5.5	
IY3-2_015	0.00	45	34	0.77	25.93 ± 0.65	0.0565 ± 0.0045	244.0 ± 6.0	242.3 ± 6.1	
IY3-2_016	0.00	29	17	0.60	26.37 ± 0.99	0.0493 ± 0.0067	240.0 ± 8.8	240.0 ± 8.8	
IY3-2_017	1.65	36	24	0.69	26.69 ± 0.82	0.0444 ± 0.0104	237.1 ± 7.2	239.0 ± 7.1	
IY3-2_018	0.00	44	31	0.72	25.80 ± 0.76	0.0523 ± 0.0055	245.1 ± 7.1	244.7 ± 7.2	
IY3-2_019	0.05	44	36	0.83	25.63 ± 0.78	0.0561 ± 0.0096	246.7 ± 7.4	245.2 ± 7.1	
IY3-2_020	0.00	59	47	0.83	25.56 ± 0.68	0.0578 ± 0.0041	247.4 ± 6.5	245.4 ± 6.5	
IY3-2_021	0.19	30	17	0.60	26.26 ± 0.94	0.0441 ± 0.0105	241.0 ± 8.5	241.4 ± 8.2	
IY3-2_022	0.00	62	51	0.84	25.21 ± 0.70	0.0496 ± 0.0041	250.8 ± 6.9	250.8 ± 6.9	
IY3-2_023	0.00	56	43	0.80	25.69 ± 0.64	0.0477 ± 0.0046	246.2 ± 6.0	246.2 ± 6.0	
IY3-2_024	0.00	50	41	0.85	26.14 ± 0.72	0.0569 ± 0.0050	242.0 ± 6.6	240.2 ± 6.7	
IY3-2_025	0.35	52	40	0.79	25.40 ± 0.78	0.0532 ± 0.0104	249.0 ± 7.5	248.4 ± 7.2	
IY3-2_026	0.46	29	14	0.49	24.09 ± 0.72	0.0486 ± 0.0103	262.2 ± 7.7	263.1 ± 7.7	
IY3-2_027	0.00	103	56	0.56	23.94 ± 0.56	0.0478 ± 0.0034	263.8 ± 6.0	263.8 ± 6.0	
IY3-2_028	0.88	31	14	0.47	27.97 ± 1.14	0.0410 ± 0.0107	226.4 ± 9.1	228.4 ± 8.9	
IY3-2_029	0.00	50	39	0.80	23.97 ± 0.62	0.0436 ± 0.0042	263.5 ± 6.7	263.5 ± 6.7	
IY3-2_030	0.00	49	26	0.55	25.30 ± 0.75	0.0533 ± 0.0054	249.9 ± 7.3	249.3 ± 7.4	
IY3-2_031	0.00	43	23	0.56	25.44 ± 0.85	0.0475 ± 0.0052	248.5 ± 8.1	248.5 ± 8.1	
IY3-2_032	0.10	300	33	0.11	25.77 ± 0.33	0.0525 ± 0.0023	245.4 ± 3.1	245.0 ± 3.1	
IY3-2_033	0.16	71	50	0.72	25.59 ± 0.67	0.0467 ± 0.0072	247.2 ± 6.3	247.5 ± 6.1	
IY3-2_034	0.00	47	34	0.76	25.25 ± 0.81	0.0504 ± 0.0045	250.4 ± 7.8	250.4 ± 7.8	
IY3-2_035	0.59	55	43	0.80	25.78 ± 0.70	0.0524 ± 0.0096	245.3 ± 6.6	244.9 ± 6.3	
IY3-2_036	0.00	33	20	0.61	24.87 ± 0.74	0.0636 ± 0.0059	254.1 ± 7.4	250.3 ± 7.5	discordant
IY3-2_037	2.19	39	29	0.77	26.28 ± 0.78	0.0357 ± 0.0130	240.8 ± 7.0	245.3 ± 6.6	
IY3-2_038	0.00	37	30	0.82	25.13 ± 0.65	0.0633 ± 0.0062	251.6 ± 6.4	247.9 ± 6.5	
IY3-2_039	0.03	56	50	0.91	25.21 ± 0.62	0.0560 ± 0.0087	250.8 ± 6.1	249.3 ± 5.8	
IY3-2_040	0.00	28	15	0.54	25.13 ± 0.80	0.0514 ± 0.0061	251.5 ± 7.9	251.5 ± 8.1	
IY3-2_041	2.50	44	35	0.82	26.49 ± 0.86	0.0277 ± 0.0125	238.9 ± 7.6	244.9 ± 7.2	
IY3-2_042	0.00	24	16	0.68	25.20 ± 0.89	0.0469 ± 0.0067	250.9 ± 8.7	250.9 ± 8.7	
IY3-2_043	0.00	86	59	0.70	25.33 ± 0.61	0.0540 ± 0.0035	249.6 ± 5.9	248.8 ± 6.0	
IY3-2_044	0.00	50	37	0.77	24.65 ± 0.65	0.0447 ± 0.0042	256.3 ± 6.6	256.3 ± 6.6	
IY3-2_045	4.25	78	40	0.52	27.56 ± 0.67	0.0382 ± 0.0092	229.8 ± 5.5	233.4 ± 5.4	
IY3-2_046	0.83	40	26	0.67	25.91 ± 0.83	0.0489 ± 0.0102	244.2 ± 7.7	244.8 ± 7.5	
IY3-2_047	0.00	29	18	0.62	26.16 ± 0.94	0.0467 ± 0.0072	241.8 ± 8.6	241.8 ± 8.6	
IY3-2_048	0.63	36	26	0.72	25.16 ± 0.89	0.0399 ± 0.0113	251.2 ± 8.7	252.8 ± 8.3	
IY3-2_049	0.00	75	56	0.76	25.38 ± 0.60	0.0527 ± 0.0039	249.2 ± 5.8	248.7 ± 5.9	
IY3-2_050	0.00	52	36	0.71	24.92 ± 0.74	0.0485 ± 0.0043	253.6 ± 7.4	253.6 ± 7.4	
IY3-2_051	0.50	37	26	0.70	25.44 ± 0.75	0.0473 ± 0.0110	248.6 ± 7.2	249.8 ± 6.9	
IY3-2_052	0.00	76	64	0.86	25.49 ± 0.59	0.0523 ± 0.0039	248.1 ± 5.7	247.7 ± 5.8	

Table A1. Continued.

Labels	$^{206}Pb_c$ (1) (%)	U (ppm)	Th (ppm)	Th/U	$^{238}U/^{206}Pb^*$ (1)	$^{207}Pb^*/^{206}Pb^*$ (1)	$^{238}U/^{206}Pb^*$ age (1) (Ma)	$^{238}U/^{206}Pb^*$ age (2) (Ma)	Remarks
IY3-2_053	0.00	90	65	0.74	26.65 ± 0.50	0.0539 ± 0.0039	237.5 ± 4.3	236.6 ± 4.5	
IY3-2_054	0.00	54	46	0.86	25.26 ± 0.64	0.0496 ± 0.0039	250.3 ± 6.2	250.3 ± 6.2	
IY3-2_055	0.00	35	26	0.75	25.04 ± 0.73	0.0440 ± 0.0054	252.4 ± 7.3	252.4 ± 7.3	
IY3-2_056	0.00	42	33	0.79	24.56 ± 0.68	0.0534 ± 0.0046	257.3 ± 7.0	256.7 ± 7.1	
IY3-2_057	0.00	30	16	0.54	25.43 ± 0.90	0.0436 ± 0.0055	248.7 ± 8.6	248.7 ± 8.6	
IY3-2_058	0.00	59	45	0.78	25.87 ± 0.69	0.0528 ± 0.0040	244.5 ± 6.4	244.0 ± 6.5	
IY3-2_059	0.12	38	31	0.84	25.28 ± 0.95	0.0443 ± 0.0115	250.1 ± 9.2	250.4 ± 8.7	
IY3-2_060	1.40	53	47	0.90	25.43 ± 0.70	0.0455 ± 0.0109	248.6 ± 6.7	250.4 ± 6.3	
IY3-2_061	1.01	48	36	0.78	26.04 ± 0.86	0.0373 ± 0.0098	242.9 ± 7.8	245.3 ± 7.6	
IY3-2_062	0.49	43	35	0.83	26.98 ± 0.80	0.0522 ± 0.0120	234.6 ± 6.8	234.2 ± 6.4	
IY3-2_063	0.00	51	40	0.80	26.30 ± 0.71	0.0473 ± 0.0041	240.6 ± 6.4	240.6 ± 6.4	
IY3-2_064	0.00	44	36	0.84	25.52 ± 0.77	0.0474 ± 0.0046	247.8 ± 7.4	247.8 ± 7.4	
IY3-2_065	0.00	35	26	0.77	25.35 ± 0.94	0.0516 ± 0.0058	249.5 ± 9.1	249.3 ± 9.2	
IY3-2_066	0.00	56	45	0.82	24.13 ± 0.60	0.0451 ± 0.0042	261.8 ± 6.4	261.8 ± 6.4	
IY3-2_067	0.47	37	28	0.78	25.53 ± 0.83	0.0523 ± 0.0110	247.7 ± 7.9	247.4 ± 7.7	
IY3-2_068	0.00	31	20	0.67	24.74 ± 0.83	0.0503 ± 0.0069	255.5 ± 8.4	255.5 ± 8.4	
IY3-2_069	0.77	33	20	0.64	25.61 ± 0.99	0.0340 ± 0.0097	246.9 ± 9.3	248.8 ± 9.1	
IY3-2_070	0.30	51	41	0.82	26.84 ± 0.80	0.0493 ± 0.0108	235.8 ± 6.9	236.3 ± 6.5	
IY3-2_071	0.00	73	64	0.90	25.50 ± 0.67	0.0541 ± 0.0046	248.0 ± 6.4	247.1 ± 6.5	
IY3-2_072	0.08	62	55	0.91	26.32 ± 0.68	0.0641 ± 0.0094	240.4 ± 6.1	236.5 ± 5.7	
IY3-2_073	0.00	35	17	0.50	25.86 ± 0.93	0.0453 ± 0.0062	244.6 ± 8.7	244.6 ± 8.7	
IY3-2_074	0.00	45	34	0.78	24.88 ± 0.84	0.0447 ± 0.0062	254.0 ± 8.4	254.0 ± 8.4	
IY3-2_075	0.91	33	18	0.55	26.44 ± 0.89	0.0446 ± 0.0125	239.3 ± 7.9	241.2 ± 7.7	
IY3-2_076	0.00	70	57	0.83	27.02 ± 0.62	0.0518 ± 0.0074	234.3 ± 5.3	234.0 ± 5.2	
IY3-2_077	0.69	51	40	0.81	25.47 ± 0.72	0.0535 ± 0.0101	248.2 ± 6.9	247.5 ± 6.6	
IY3-2_078	0.00	48	36	0.77	25.96 ± 0.79	0.0515 ± 0.0049	243.7 ± 7.3	243.6 ± 7.5	
IY3-2_079	0.00	50	38	0.78	25.21 ± 0.61	0.0512 ± 0.0049	250.7 ± 6.0	250.7 ± 6.0	
IY3-2_080	3.16	48	39	0.83	26.82 ± 0.81	0.0530 ± 0.0118	236.0 ± 7.0	235.4 ± 6.8	
IY3-2_081	1.89	47	35	0.75	26.69 ± 0.86	0.0541 ± 0.0120	237.1 ± 7.5	236.2 ± 7.2	
IY3-2_082	0.00	50	38	0.77	25.26 ± 0.73	0.0580 ± 0.0057	250.3 ± 7.1	248.2 ± 7.2	
IY3-2_083	0.73	37	23	0.65	27.30 ± 0.93	0.0532 ± 0.0109	231.9 ± 7.8	231.3 ± 7.6	
IY3-2_084	0.00	50	38	0.78	26.78 ± 0.82	0.0479 ± 0.0044	236.3 ± 7.1	236.3 ± 7.1	
IY3-2_085	1.00	50	42	0.87	26.31 ± 0.66	0.0471 ± 0.0096	240.4 ± 6.0	241.6 ± 5.7	
IY3-2_086	2.23	45	30	0.69	27.41 ± 0.95	0.0384 ± 0.0113	231.0 ± 7.9	234.5 ± 7.7	
IY3-2_087	0.00	30	16	0.54	25.24 ± 1.02	0.0545 ± 0.0070	250.4 ± 10.0	249.4 ± 10.2	
IY3-2_088	0.00	38	24	0.64	26.06 ± 0.92	0.0563 ± 0.0066	242.7 ± 8.4	241.2 ± 8.6	
IY3-2_089	1.36	38	17	0.46	25.68 ± 0.96	0.0410 ± 0.0100	246.2 ± 9.0	249.3 ± 9.0	
IY3-2_090	0.41	37	29	0.81	25.41 ± 0.91	0.0482 ± 0.0123	248.9 ± 8.7	249.8 ± 8.3	
IY3-2_091	0.00	36	24	0.67	26.39 ± 0.91	0.0499 ± 0.0059	239.8 ± 8.1	239.8 ± 8.1	
IY3-2_092	0.44	39	26	0.69	25.69 ± 0.93	0.0507 ± 0.0106	246.2 ± 8.7	246.3 ± 8.5	
IY3-2_093	0.33	50	39	0.79	26.32 ± 0.77	0.0421 ± 0.0097	240.4 ± 6.9	241.2 ± 6.6	
IY3-2_094	0.00	47	37	0.80	24.89 ± 0.79	0.0610 ± 0.0065	253.9 ± 7.9	250.9 ± 8.1	
IY3-2_095	0.00	56	46	0.83	25.11 ± 0.71	0.0542 ± 0.0046	251.7 ± 7.0	250.8 ± 7.1	
IY3-2_096	0.87	88	83	0.97	25.87 ± 0.65	0.0412 ± 0.0103	244.5 ± 6.1	246.6 ± 5.5	
IY3-2_097	0.00	34	26	0.79	23.21 ± 0.81	0.0456 ± 0.0061	271.9 ± 9.3	271.9 ± 9.3	
IY3-2_098	0.00	37	26	0.73	25.14 ± 0.88	0.0531 ± 0.0069	251.4 ± 8.6	250.8 ± 8.9	
IY3-2_099	0.00	62	43	0.71	25.37 ± 0.69	0.0501 ± 0.0039	249.2 ± 6.6	249.2 ± 6.6	
IY3-2_100	1.36	90	88	1.00	26.82 ± 0.70	0.0470 ± 0.0113	236.0 ± 6.1	237.1 ± 5.5	
IY3-2_101	1.82	60	45	0.76	25.42 ± 0.80	0.0351 ± 0.0102	248.8 ± 7.7	253.3 ± 7.4	
IY3-2_102	1.22	48	25	0.52	25.86 ± 0.83	0.0385 ± 0.0094	244.6 ± 7.7	247.6 ± 7.4	
IY4-1_001	0.00	42	23	0.56	24.91 ± 0.83	0.0425 ± 0.0053	253.7 ± 8.3	253.7 ± 8.3	
IY4-1_002	2.45	114	110	0.99	27.70 ± 0.78	0.0322 ± 0.0107	228.6 ± 6.3	233.8 ± 6.0	
IY4-1_003	0.00	81	69	0.87	27.76 ± 1.06	0.0529 ± 0.0069	228.1 ± 8.5	227.5 ± 8.7	
IY4-1_004	0.06	98	90	0.94	28.36 ± 0.83	0.0541 ± 0.0108	223.4 ± 6.5	222.5 ± 6.2	
IY4-1_005	1.17	33	19	0.61	27.13 ± 1.28	0.0456 ± 0.0149	233.3 ± 10.8	234.8 ± 10.7	
IY4-1_006	0.00	81	64	0.81	26.76 ± 0.76	0.0490 ± 0.0048	236.5 ± 6.6	236.5 ± 6.6	
IY4-1_007	0.00	90	65	0.74	26.31 ± 0.64	0.0483 ± 0.0041	240.5 ± 5.7	240.5 ± 5.7	
IY4-1_008	2.03	86	78	0.93	27.47 ± 0.85	0.0421 ± 0.0124	230.5 ± 7.0	233.0 ± 6.5	
IY4-1_009	0.74	82	73	0.91	28.78 ± 0.93	0.0502 ± 0.0119	220.2 ± 7.0	220.3 ± 6.6	
IY4-1_010	0.23	93	84	0.93	27.52 ± 0.84	0.0477 ± 0.0091	230.1 ± 6.9	230.6 ± 6.5	
IY4-1_011	0.00	42	31	0.77	25.42 ± 0.84	0.0610 ± 0.0076	248.7 ± 8.1	245.7 ± 8.3	
IY4-1_012	1.12	64	45	0.72	25.94 ± 0.85	0.0579 ± 0.0122	243.8 ± 7.8	241.8 ± 7.4	
IY4-1_013	0.00	39	24	0.63	27.70 ± 0.99	0.0556 ± 0.0077	228.6 ± 8.0	227.3 ± 8.3	

Table A1. Continued.

Labels	$^{206}Pb_c$ (1) (%)	U (ppm)	Th (ppm)	Th/U	$^{238}U/^{206}Pb^{*}$ (1)	$^{207}Pb^{*}/^{206}Pb^{*}$ (1)	$^{238}U/^{206}Pb^{*}$ age (1) (Ma)	$^{238}U/^{206}Pb^{*}$ age (2) (Ma)	Remarks
IY4-1_014	4.87	32	19	0.60	27.44 ± 1.29	0.0418 ± 0.0202	230.8 ± 10.6	233.4 ± 10.6	
IY4-1_015	0.00	47	40	0.87	24.57 ± 0.86	0.0474 ± 0.0048	257.2 ± 8.8	257.2 ± 8.8	
IY4-1_016	0.00	153	184	1.23	25.35 ± 0.51	0.0570 ± 0.0033	249.4 ± 4.9	247.7 ± 5.0	
IY4-1_017	0.00	97	99	1.05	26.44 ± 0.62	0.0464 ± 0.0037	239.3 ± 5.5	239.3 ± 5.5	
IY4-1_018	0.00	46	33	0.74	27.28 ± 0.99	0.0458 ± 0.0066	232.1 ± 8.3	232.1 ± 8.3	
IY4-1_019	1.28	39	25	0.65	26.77 ± 0.98	0.0518 ± 0.0137	236.4 ± 8.5	236.2 ± 8.2	
IY4-1_020	0.00	49	28	0.59	26.89 ± 1.01	0.0628 ± 0.0066	235.4 ± 8.6	232.0 ± 8.7	
IY4-1_021	0.00	71	66	0.95	26.37 ± 0.71	0.0439 ± 0.0043	240.0 ± 6.3	240.0 ± 6.3	
IY4-1_022	0.07	30	12	0.41	26.86 ± 1.00	0.0421 ± 0.0107	235.6 ± 8.6	235.8 ± 8.3	
IY4-1_023	0.17	30	15	0.52	26.53 ± 1.13	0.0604 ± 0.0133	238.5 ± 10.0	235.8 ± 9.8	
IY4-1_024	0.00	59	33	0.58	27.46 ± 0.74	0.0494 ± 0.0053	230.6 ± 6.1	230.6 ± 6.1	
IY4-1_025	1.81	55	43	0.80	29.14 ± 0.97	0.0475 ± 0.0114	217.5 ± 7.1	218.3 ± 6.9	
IY4-1_026	0.49	56	45	0.83	26.90 ± 0.81	0.0644 ± 0.0114	235.3 ± 7.0	231.4 ± 6.5	
IY4-1_027	1.71	67	61	0.93	27.59 ± 0.92	0.0483 ± 0.0123	229.6 ± 7.5	230.3 ± 7.2	
IY4-1_028	3.74	45	37	0.84	26.78 ± 0.99	0.0538 ± 0.0164	236.3 ± 8.6	235.5 ± 8.2	
IY4-1_029	3.02	48	39	0.83	24.10 ± 0.83	0.1089 ± 0.0142	262.1 ± 8.8	243.8 ± 8.1	discordant
IY4-1_030	0.00	66	56	0.87	26.98 ± 0.85	0.0429 ± 0.0055	234.6 ± 7.2	234.6 ± 7.2	
IY4-1_031	2.81	42	30	0.75	26.38 ± 1.07	0.0460 ± 0.0152	239.8 ± 9.5	241.3 ± 9.3	
IY4-1_032	0.00	50	43	0.88	26.34 ± 0.81	0.0451 ± 0.0061	240.2 ± 7.2	240.2 ± 7.2	
IY4-1_033	1.10	86	81	0.97	28.09 ± 0.81	0.0468 ± 0.0092	225.5 ± 6.4	226.5 ± 6.2	
IY4-1_034	1.36	111	103	0.96	29.75 ± 0.85	0.0462 ± 0.0113	213.1 ± 6.0	214.3 ± 5.6	
IY4-1_035	0.00	38	19	0.50	27.58 ± 1.19	0.0412 ± 0.0071	229.6 ± 9.8	229.6 ± 9.8	
IY4-1_036	0.00	49	31	0.65	28.52 ± 1.00	0.0446 ± 0.0056	222.1 ± 7.6	222.1 ± 7.6	
IY4-1_037	0.00	57	47	0.84	25.65 ± 0.90	0.0462 ± 0.0059	246.5 ± 8.5	246.5 ± 8.5	
IY4-1_038	1.20	47	30	0.67	28.44 ± 1.21	0.0413 ± 0.0133	222.8 ± 9.3	225.3 ± 9.1	
IY4-1_039	0.00	129	127	1.01	27.05 ± 0.66	0.0436 ± 0.0042	234.0 ± 5.6	234.0 ± 5.6	
IY4-1_040	2.24	96	85	0.90	27.97 ± 1.03	0.0488 ± 0.0136	226.5 ± 8.2	227.0 ± 7.9	
IY4-1_041	0.98	51	41	0.82	28.21 ± 1.34	0.0535 ± 0.0161	224.6 ± 10.5	223.8 ± 10.2	
IY4-1_042	0.00	104	97	0.96	26.66 ± 0.89	0.0565 ± 0.0049	237.4 ± 7.8	235.8 ± 7.9	
IY4-1_043	2.36	52	37	0.74	28.57 ± 1.17	0.0260 ± 0.0157	221.8 ± 9.0	227.1 ± 8.4	
IY4-1_044	1.73	42	26	0.64	27.71 ± 1.10	0.0535 ± 0.0150	228.5 ± 8.9	227.8 ± 8.9	
IY4-1_045	0.00	33	20	0.63	29.06 ± 1.43	0.0481 ± 0.0137	218.1 ± 10.6	218.1 ± 10.6	
IY4-1_046	0.00	47	34	0.74	27.90 ± 1.00	0.0505 ± 0.0070	227.0 ± 8.0	227.0 ± 8.0	
IY4-1_047	1.13	68	57	0.86	27.50 ± 1.01	0.0409 ± 0.0121	230.2 ± 8.3	232.8 ± 7.9	
IY4-1_048	0.00	71	59	0.86	27.23 ± 0.89	0.0509 ± 0.0065	232.5 ± 7.5	232.5 ± 7.7	
IY4-1_049	0.00	32	21	0.67	26.15 ± 1.28	0.0607 ± 0.0125	241.9 ± 11.6	239.0 ± 12.0	
IY4-1_050	0.01	64	58	0.93	27.94 ± 1.21	0.0595 ± 0.0154	226.7 ± 9.6	224.2 ± 9.1	
IY4-1_051	0.64	51	8	0.16	26.52 ± 1.02	0.0367 ± 0.0085	238.6 ± 9.0	240.1 ± 8.9	
IY4-1_052	0.00	33	23	0.70	27.15 ± 1.03	0.0421 ± 0.0072	233.2 ± 8.7	233.2 ± 8.7	
IY4-1_053	0.00	82	79	0.98	27.83 ± 0.99	0.0536 ± 0.0060	227.6 ± 7.9	226.8 ± 8.1	
IY4-1_054	2.76	96	92	0.99	29.91 ± 0.86	0.0577 ± 0.0124	212.0 ± 6.0	210.1 ± 5.7	
IY4-1_055	0.00	83	76	0.93	28.52 ± 0.81	0.0621 ± 0.0050	222.1 ± 6.2	219.0 ± 6.3	discordant
IY4-1_056	0.73	41	28	0.70	27.96 ± 1.21	0.0424 ± 0.0130	226.5 ± 9.6	228.2 ± 9.3	
IY4-1_057	0.00	49	25	0.53	29.12 ± 1.26	0.0404 ± 0.0060	217.6 ± 9.3	217.6 ± 9.3	
IY4-1_058	0.00	68	56	0.84	29.39 ± 1.06	0.0633 ± 0.0073	215.7 ± 7.7	212.3 ± 7.8	
IY4-1_059	0.00	75	41	0.56	25.23 ± 0.85	0.0424 ± 0.0049	250.6 ± 8.3	250.6 ± 8.3	
IY4-1_060	0.64	47	25	0.55	27.97 ± 1.29	0.0410 ± 0.0125	226.4 ± 10.3	227.9 ± 10.0	
IY4-1_061	0.00	47	37	0.80	28.41 ± 1.15	0.0535 ± 0.0059	223.0 ± 8.9	222.2 ± 9.0	
IY4-1_062	0.00	147	158	1.11	26.83 ± 0.66	0.0561 ± 0.0038	235.9 ± 5.7	234.4 ± 5.8	
IY4-1_063	0.05	46	33	0.72	26.77 ± 1.10	0.0629 ± 0.0135	236.4 ± 9.5	233.0 ± 9.3	
IY4-1_064	0.00	83	73	0.90	26.13 ± 0.82	0.0459 ± 0.0047	242.1 ± 7.4	242.1 ± 7.4	
IY4-1_065	0.00	59	50	0.87	27.51 ± 1.12	0.0635 ± 0.0073	230.1 ± 9.2	226.5 ± 9.3	
IY4-1_066	0.00	54	42	0.80	24.61 ± 0.93	0.0612 ± 0.0064	256.7 ± 9.6	253.6 ± 9.7	
IY4-1_067	0.00	58	26	0.47	23.85 ± 0.79	0.0679 ± 0.0071	264.8 ± 8.6	259.5 ± 8.8	discordant
IY4-1_068	0.00	33	17	0.53	28.20 ± 1.20	0.0453 ± 0.0100	224.7 ± 9.4	224.7 ± 9.4	
IY4-1_069	0.33	44	27	0.63	25.99 ± 1.01	0.0543 ± 0.0133	243.4 ± 9.3	242.4 ± 9.2	
IY4-1_070	3.16	39	28	0.74	28.71 ± 1.28	0.0241 ± 0.0145	220.7 ± 9.6	227.8 ± 9.4	
IY4-1_071	0.32	74	71	0.99	26.13 ± 0.88	0.0452 ± 0.0115	242.1 ± 8.0	242.9 ± 7.5	
IY4-1_072	0.00	36	22	0.62	29.15 ± 1.15	0.0665 ± 0.0094	217.4 ± 8.4	213.1 ± 8.7	

Errors are 1-sigma; Pb_c and Pb^{*} indicate the common and radiogenic portions, respectively.
(1) Common Pb corrected by assuming $^{206}Pb/^{238}U$-$^{208}Pb/^{232}Th$ age-concordance
(2) Common Pb corrected by assuming $^{206}Pb/^{238}U$-$^{207}Pb/^{235}U$ age-concordance